

Available online at [www.sciencedirect.com](http://www.sciencedirect.com)

ScienceDirect

journal homepage: [www.elsevier.com/locate/ijhydene](http://www.elsevier.com/locate/ijhydene)

## Short Communication

# Effect of anode morphology on the performance of thin film solid oxide fuel cell with PEALD YSZ electrolyte



Taehyun Park <sup>a,1</sup>, Gu Young Cho <sup>a,1</sup>, Yoon Ho Lee <sup>a</sup>,  
 Waqas Hassan Tanveer <sup>a</sup>, Wonjong Yu <sup>a</sup>, Yeageun Lee <sup>a</sup>, Yusung Kim <sup>a</sup>,  
 Jihwan An <sup>b,\*\*</sup>, Suk Won Cha <sup>a,\*</sup>

<sup>a</sup> Department of Mechanical and Aerospace Engineering, Seoul National University, 1 Gwanak-ro, Gwanak-gu, Seoul, 08826, Republic of Korea

<sup>b</sup> Manufacturing Systems and Design Engineering Programme, Seoul National University of Science and Technology, 232 Gongneung-ro, Nowon-gu, Seoul, 01811, Republic of Korea

## ARTICLE INFO

## Article history:

Received 28 December 2015

Received in revised form

4 April 2016

Accepted 13 April 2016

Available online 12 May 2016

## Keywords:

Solid oxide fuel cell (SOFC)

Thin film

Plasma-enhanced atomic layer deposition (PEALD)

Yttria-stabilized zirconia (YSZ)

Anodic aluminum oxide (AAO)

## ABSTRACT

Thin film solid oxide fuel cells (SOFCs) with Pt anode, yttria-stabilized zirconia (YSZ) electrolyte, and Pt cathode were fabricated based on nano-porous substrate. Pt and YSZ were deposited using sputter and plasma-enhanced atomic layer deposition (PEALD), respectively. Here, two types of Pt anode, i.e., dense and porous, were prepared to compare the performances of the fuel cells. The performance of the fuel cell with the porous Pt anode showed higher peak power density (194 mW/cm<sup>2</sup>) than that with the dense Pt anode (178 mW/cm<sup>2</sup>) at 500 °C. Through the analyses via scanning electron microscopy and electrochemical impedance spectroscopy (EIS), it was found that the increase of the performance was attributed to the enhanced supply of the hydrogen into the porous anode and resulting enhancement of charge transfer and mass transport. In the EIS results, the anodic charge transfer resistance of the fuel cell with the dense Pt anode was higher than that of the porous Pt anode, even though the porous Pt anode is thicker than the dense Pt anode. The result from a high-resolution transmission electron microscopy and electron-dispersive spectroscopy images showed that anodic pores were slightly filled with YSZ due to the low conformality of PEALD, resulting in the additional formation of triple phase boundaries.

© 2016 Hydrogen Energy Publications LLC. Published by Elsevier Ltd. All rights reserved.

\* Corresponding author.

\*\* Corresponding author.

E-mail addresses: [jihwanan@seoultech.ac.kr](mailto:jihwanan@seoultech.ac.kr) (J. An), [swcha@snu.ac.kr](mailto:swcha@snu.ac.kr) (S.W. Cha).

<sup>1</sup> Both authors contributed equally to this work.

<http://dx.doi.org/10.1016/j.ijhydene.2016.04.092>

0360-3199/© 2016 Hydrogen Energy Publications LLC. Published by Elsevier Ltd. All rights reserved.

## Introduction

Solid oxide fuel cell (SOFC) is one of the promising fuel cell types due to fuel flexibility, material selectivity, and high energy conversion efficiency [1,2]. In SOFCs, yttria-stabilized zirconia (YSZ) has been widely used as an electrolyte material because it is cheap and chemically stable [3]. However, YSZ has relatively low ionic conductivity, thus the SOFC with YSZ electrolyte requires high operating temperature (>700 °C). In this temperature regime, however, SOFC would have several problems such as long start-up time, difficult sealing, and the limitation of choosing component materials. Many researches about SOFCs, therefore, have focused on lowering the operating temperature to intermediate range (450–600 °C) [4].

One method to lower the operating temperature is to make an electrolyte as thin as possible. It is because the large portion of the performance loss stems from the ohmic loss due to the low ionic conduction of ceramic electrolyte. Because the ohmic resistance is proportional to the thickness of the electrolyte, the ohmic loss can be reduced by making the electrolyte extremely thin (<1 μm) by using thin film deposition techniques. Several studies recently have reported that the performance of the SOFC is significantly enhanced when electrodes and electrolytes are fabricated in ultra-thin films (<100 nm) [3,5–9]. These thin films have been fabricated by utilizing sputter, pulsed laser deposition, or atomic layer deposition (ALD) systems. However, most of these researches have utilized Si wafer-based architectures. These are not suitable for large-area fabrication and commercialization because the structure is mechanically very fragile due to the free-standing membrane electrode assembly with the extremely high aspect ratio (thickness vs. width of the fuel cell).

In order to resolve the issues associated with Si wafer-based architectures, anodic aluminum oxide (AAO) was adopted as substrate and thin film electrode and electrolyte were deposited on it [9–18]. This approach is advantageous in enlarging the reactive area. However, it requires thicker electrolyte than that in Si wafer-based cells owing to the roughness of the porous surface on AAO, which may result in pinholes. Our previous researches therefore have used relatively thick and dense anodes with the thickness of 300–500 nm [11,13–15], which is thicker than that of Si wafer-based cells (<100 nm). Recently, Hong et al. successfully demonstrated the thin film SOFC with 180 nm thick YSZ deposited on AAO by using ALD [18]. They adopted ‘multi-layered’ scheme to resolve pinhole issues by combinatorial sputtering deposition of a Pt. It showed maximum performance of 380 mW/cm<sup>2</sup> at 450 °C, which is comparable to the performance of Si wafer-based cells. Ji et al. reported the feasibility of thinner YSZ single electrolyte (70 nm) on a single Pt anode structure on AAO with larger reactive area (1 × 1 mm<sup>2</sup>), by combining sputtered electrode and plasma-enhanced ALD (PEALD) electrolytes [14]. This research also shows the feasibility of thin film SOFC fabricated on nanoporous AAO with the single PEALD YSZ layer as an electrolyte. Most of these researches, however, have focused on the electrolyte materials and structures of AAO-supported cells,

while the study on the effect of electrode structure has rarely been reported. Park et al. reported the effect of this anode porosity on the performance of thin film SOFCs. It showed the morphological details of the anode and resulting performances but the power density was not high due to the fabrication of the YSZ electrolyte via sputtering [12].

In this study, we report the effect of anode morphology, i.e., dense and porous, on the performance of AAO-supported thin film SOFC. Particularly, YSZ was used as an electrolyte and deposited on the Pt anode by PEALD. The fuel cell with the porous Pt anode shows the maximal power density of 194 mW/cm<sup>2</sup>. It is higher than that with the dense Pt anode (178 mW/cm<sup>2</sup>) on AAO substrate. The corresponding impedance spectra show that the increased performance in the porous Pt anode cell is due to lower charge transfer resistance and mass transport resistance, which is also supported by energy-dispersive spectroscopy (EDS) and transmission electron microscopy (TEM) images. The result here also implies that electrode porosity is essential in achieving the high-performance in thin film SOFCs when the electrolyte is prepared by PEALD on AAO-substrate.

## Experimental

### Preparation of the fuel cell

The AAO (Synkera Co., USA) with the pore size of 80 nm was used as a substrate for the deposition of thin film SOFC. Pt anode was first deposited on this AAO by sputter (AT12, A-Tech System Co., Republic of Korea). The Pt anodes were prepared as two morphologies: porous and dense films. The morphology was controlled by differentiating the pressure of argon gas inside the sputter chamber: 0.67 Pa for dense and 4 Pa for porous anode. The dense Pt anode of 300 nm and porous Pt anode of 450 nm were deposited. DC sputtering power for the Pt was 200 W for both porous and dense cases. On top of each Pt anode, YSZ was deposited by utilizing commercial PEALD system (Atomic Premium, CN1 Co., Republic of Korea) with a radio-frequency plasma generator. The set temperatures were as follows: a substrate of 250 °C, canister of yttrium precursor of 150 °C (Tris-(methylcyclopentadienyl)yttrium, RND Korea Co., Republic of Korea), supply line of yttria precursor of 165 °C, canister of zirconium precursor of 50 °C (Tetrakis-(dimethylamido)zirconium, RND Korea Co., Republic of Korea), supply line of zirconia precursor of 70 °C. The repetitive step of zirconia-deposition was as follows: 3 s of zirconium precursor pulsing, 40 s of purging by argon gas, 1 s of oxygen gas pulsing, 3 s of oxygen gas pulsing with plasma, and 40 s of purging by argon gas. The yttria-deposition was as follows: 3 s of yttrium precursor pulsing, 75 s of purging by argon gas, 1 s of oxygen gas pulsing, 3 s of oxygen gas pulsing with plasma, and 75 s of purging by argon gas, all in sequence. The doping rate of the yttria was controlled by varying the ratio of the number of each zirconium and yttrium deposition cycle. The investigated ratio of the PEALD cycles for YSZ showing the yttria of around 8 mol% was 7 (zirconia): 1 (yttria). Total 1000 cycles of the PEALD YSZ resulted in the film thickness of 150 nm. On top of it, Pt cathode was deposited by sputter again. The DC sputtering

power, pressure of argon gas for the cathode were 100 W and 12 Pa, respectively. In all sputtering processes, target–substrate distances were same as 80 mm.

### Performance measurement

The as-fabricated thin film SOFC was mounted on a specially designed test station, described elsewhere [15]. The fuel cell was first attached on the test station using a silver paste (Aremco 597A, Aremco Products Co., USA) to collect the generated current and voltage to an external circuit and electrochemical measurement system (Solartron 1260/1287, Solartron Analytical Co., UK). On the silver paste, a sealant (Aremco CP4010, Aremco Products Co., USA) was applied to ensure sealability between the cell and the test station. After drying the silver paste and sealant, it was placed into a customized electric furnace with a small hole for the cell-measurement. It was heated up and kept to 500 °C during test. The pre-heated dry hydrogen of 99.99% purity was supplied to the anode of the fuel cell with the volumetric flow rate of 0.5 cm<sup>3</sup>/s, which is the abundant amount for the fuel cell operation stoichiometrically. Air was supplied by just exposing the Pt cathode directly to the ambient air in the furnace. Current–voltage (I–V) characteristics were measured through potentiodynamic mode with the voltaic scanning rate of 0.03 V/s. Right after measuring the I–V, electrochemical impedance at 0.5 V was measured. Sinusoidal voltage input with the amplitude of 0.03 V and the frequency range from 10<sup>5</sup> to 2 Hz was applied and resulting current behavior was monitored.

### Characterization via microscopies

The images of the surface morphologies of the fuel cell were obtained through field-emission scanning electron microscopy

(FESEM, S-4800, Hitachi Co., Japan) and the cross-sectional images through focused ion beam-SEM (FIB-SEM, Quanta 3D FEG, FEI Co., USA) with the magnification of 10<sup>5</sup> and the operating voltage of 5 kV. The surfaces of YSZ film on Pt anode and Pt cathode on YSZ film were visualized as FESEM images and compared. The roughness of each Pt anode was measured using atomic force microscope (AFM, XE100, Park Systems Co., Republic of Korea). The coverage and infiltration of the PEALD YSZ into nano-pores were investigated through high-resolution transmission electron microscopy (HRTEM, JEM-2100F, JEOL, Japan) with EDS function.

## Results and discussion

Fig. 1(a) and (b) show the cross-sectional view of the prepared thin film SOFCs on AAO. The columnar pore structures of the AAO substrate are clearly visualized, thus it can be expected that there would be no performance loss due to the hydrogen supply through the pores of AAO. There have been several researches about thin film SOFCs based on the AAO with same pore size and all the mass transport issues in those literatures were associated with dense anode, not from the structural limitation of the AAO [12]. The difference in porosity between two fuel cells is also clearly seen in Fig. 1(c) and (d) that the anode in Fig. 1(d) is more porous than Fig. 1(c). The Pt cathodes in both Fig. 1(a) and (b) are porous, as expected from the experimental conditions (the highest argon pressure among all sputtering processes) [19]. The surface morphologies of the Pt cathodes in Fig. 1(a) and (b) are indicated in Fig. S1(a) and (c).

In the previous researches about thin film SOFCs based on this nano-porous substrate, dense anode has been generally adopted as the anode is prepared by sputtering. It is because the sputtered porous metal anode has more pinholes than the dense one, as indicated in Fig. 1. Chang et al. reported that the

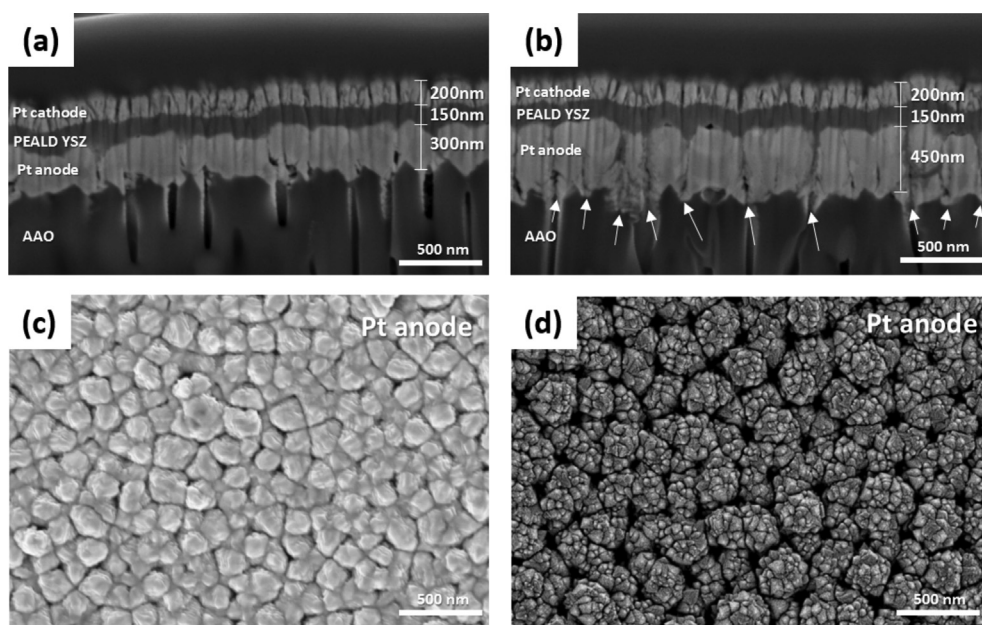


**Fig. 1** – FIB-SEM images of thin film SOFCs fabricated on nano-porous AAO substrate with (a) dense and (b) porous Pt anode. (c) and (d) show the surface images of the dense and porous Pt anodes on AAO, respectively. The magnification here is 10<sup>5</sup>.

sputtered porous Pt anode deposited at the same conditions in this study has three times rougher surface than dense Pt anode [19]. Since the diameter of the pores in AAO is 80 nm and the pores of the Pt anode are even smaller than 80 nm, the pores are likely to be partially clogged by the sputtered anode. It makes final pinholes grow from the pores of the AAO (indicated by white arrows in Fig. 1(b)). It could cause the electrical shortage through the cells. Same phenomenon was observed and discussed elsewhere [12]. We therefore tried to fabricate the porous Pt anode thicker (450 nm) than the dense one (300 nm) in order to avoid such pinholes. The reason the thicknesses of the dense and porous anode are different is that the mass transport loss was found in thicker than 300 nm in dense and 450 nm in porous Pt anodes in the previous research [12]. This study thereby started investigating the performance at the maximal thicknesses with no mass transport loss (Too thin anode is reversely detrimental due to the increased ohmic resistance). However, Ha et al. showed that it is also the case in the dense Pt anode that even a finer surface by dense Pt anode still has the problem of the generation of pinholes [11]. It means that thicker electrolyte than that in silicon wafer-based thin film SOFCs is needed if thin film SOFCs are desired to be fabricated on the nano-porous substrate. Indeed, previous researches showed that the electrolytes should be thicker than 300 nm to prevent the electrical shortage stemming from the pinholes in electrolyte layers [10–13,15–17]. However, Hong et al. recently reported that it is possible to realize thin film SOFCs with 180 nm thick YSZ electrolyte on the AAO by fabricating a combinatorial Pt anode (porous Pt on dense Pt layer). It showed the highest performance among thin film SOFCs based on the porous substrate at 450 °C [18]. Notable point of this result is that the electrolyte did not show the electrical shortage, i.e., no significant pinhole issue, even with the porous anode. Accordingly, we thought that the extremely uniform and conformal nature of PEALD films compared to thin films fabricated by other techniques, including thermal ALD, might also enable such difference in manufacturing flexibility.

The surfaces of Pt cathode and PEALD YSZ in this study are indicated in Fig. S1. Severe pinholes are not observable in Fig. S1(b) and (d). It means that the pinholes in the Pt anodes are almost completely covered with the PEALD YSZ layer. The PEALD YSZ shows good polycrystallinity, which coincides with the previous reports [3,14]. The surfaces of the Pt cathodes in Fig. S1(a) and (c) show well-defined pores (gaps between Pt grains), which can also be seen in Fig. 1(a) and (b).

Fig. 2(a) shows the polarization curves of the fuel cells. The peak power density of the fuel cell with the porous Pt anode is higher (194 mW/cm<sup>2</sup>) than that with the dense Pt anode (178 mW/cm<sup>2</sup>). Open-circuit voltages (OCVs) for the porous and dense Pt anode cases are 1.13 and 1.10 V, respectively. Although the OCVs for both cases are very close to Nernst voltage (1.18 V at 500 °C), the voltage difference of 0.03 V means ~2.5-fold difference of hydrogen concentrations according to Nernst equation (there is no difference of cathode structures nor the supply of the air in both fuel cells, meaning that this voltage difference should come from the concentration of hydrogen) [20]. Therefore, this difference is attributed to the difference of the anodic porosity between two fuel cells. As shown in Fig. 1(c) and (d), it is clear that almost all the

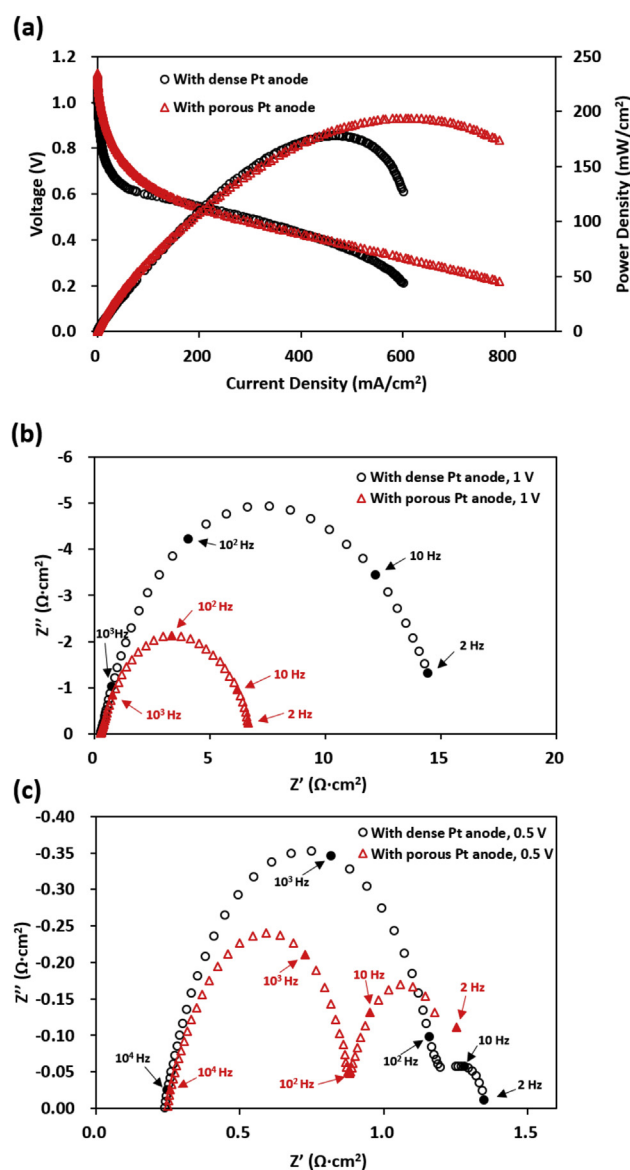


**Fig. 2** – (a) I–V and corresponding power density curves of thin film SOFCs fabricated on AAO. (b) Electrochemical impedance spectra of the cells at 1 and 0.5 V. (c) indicates magnified spectra of the impedances at 0.5 V in (b). Red and black marks in all figures indicate the fuel cells with the porous and dense Pt anode, respectively. (For interpretation of the references to colour in this figure legend, the reader is referred to the web version of this article.)

pores remain unclogged in Fig. 1(d) while many columnar pores are clogged by the dense Pt anode in Fig. 1(c), which may have caused the decrease of hydrogen concentration at the anode. Same tendency of the variation of the OCV can be found elsewhere [12]. In low current density range (0–150 mA/cm<sup>2</sup>), there is a remarkable difference of the activation loss between two fuel cells: the cell with the dense Pt anode shows much sharper drop of the voltage compared to that with the porous anode. This type of the loss is related to four parameters: reaction area (TPB), concentrations of reactants,

temperature, and activation energy barrier [17]. Here, the anodic TPB in the fuel cell is the site where the Pt anode, PEALD YSZ and hydrogen meet altogether. Considering that the other components (YSZ electrolyte and Pt cathode) are same, the difference of two fuel cells should have come from the Pt anode. It is speculated that this result is attributed to the differences of the area of TPBs: because the porous Pt anode has larger electrochemical surface area (ECSA) than the dense Pt anode according to Fig. 1(c) and (d), it generates more TPBs than the dense anode. It means that the effective ECSA in the fuel cell with the porous Pt anode is larger than that with the dense anode. This may have led to the decrease of the charge transfer resistance of the fuel cell on porous Pt anode. That is why twice larger charge transfer resistance at low current density (corresponding to 1 V) is shown in the case with the dense Pt anode in Fig. 2(b). It also matches well with the impedance spectra in Fig. 2(c) that the diameter of the half-circle at high frequency range, known as an anodic charge transfer resistance, is bigger than that with the porous Pt anode. However, intriguing behavior is observed in the low frequency range in Fig. 2(c): the second half-circle of the fuel cell with the porous Pt anode is reversely bigger than that with the dense Pt anode. It is speculated that this result is due to the difference of the ECSAs between two fuel cells. Although the porous Pt anode seems rougher in nanoscale according to Fig. 1(c) and (d), the root-mean square (RMS) value of the dense anode, which was obtained from the AFM results shown in Fig. S2, was 19.8 nm. It is higher than the RMS value of the porous Pt anode (13.53 nm). Considering that this nanostructure was covered by the PEALD YSZ, the microscale roughness became dominant and it would affect the ECSAs of two fuel cells. It is believed that the porous Pt anode mitigates the roughness of the support more than the dense Pt anode does, which can be also found elsewhere [12].

In high current density range ( $>300$  mA/cm<sup>2</sup>), mass transport loss in the fuel cell with the dense Pt anode is higher as current density increases although the thickness of dense Pt anode (300 nm) is thinner than that of porous one (450 nm). This phenomenon seems to be closely related to the mass transport of the reactant gas, i.e., hydrogen gas, into the

anode: the reactant gas seems to have been disturbed more in the dense structure. Aforementioned difference in OCV is also related to the mass transport loss here because not only the mass transport loss but also open-circuit voltage is a function of reactant concentration [20].

Cross-sectional TEM images and corresponding EDS mapping results in Fig. 3 further show that the enhanced performance in the fuel cell on the porous Pt anode may be due to the improvement in charge transfer and mass transport at the anode. Separate maps of the Zr and Pt are indicated in Fig. S3. Pores of dense Pt anode (Fig. 3(a)) are shown to be physically blocked so that TPB was not properly formed and the access of hydrogen gas may not have been facilitated. In contrast, pores of porous Pt anode (Fig. 3(b)) look physically open and YSZ was observed even in the pores, i.e., the atomic percentage of Zr was  $>20\%$  at point 2 and 3 (Table 1, detailed information in Table S1–S3). Here, because the intensity of Zr is low, it is thought that the YSZ was deposited slightly in the surfaces of the pores. One of the characteristics of PEALD is that it is less conformal deposition technique than thermal ALD because the infiltration of the ions and radicals in plasma into the pores is less active than that of thermal ALD [21]. That is why we think that the PEALD YSZ inside the pores may have formed in porous structure. It implies that TPB could be formed in larger area along the open transport route for hydrogen gas.

## Conclusion

Two types of the Pt anodes, i.e., dense and porous anodes, were prepared and tested for thin film SOFCs on AAO substrates. The peak power density of the fuel cell with the porous Pt anode was 194 mW/cm<sup>2</sup>, which is higher than 178 mW/cm<sup>2</sup> from the fuel cell with the dense Pt anode. The higher performance of the fuel cell with porous Pt anode was due to the larger porosity resulting in improved hydrogen supply to reaction sites and also due to the high TPB density. In conclusion, an anode morphology with enough porosity is required to maximize the utility of PEALD for thin film SOFCs

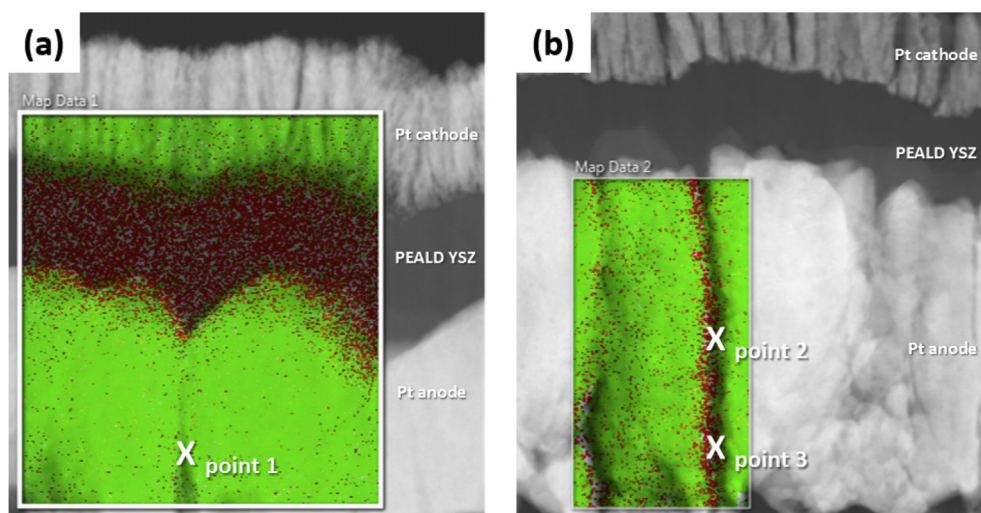


Fig. 3 – TEM images of the fuel cells with (a) dense and (b) porous Pt anode with EDS mapping overlaid on it.

**Table 1 – Compositions of Zr and Pt at three points indicated in Fig. 3 measured by TEM-EDS.**

	Element	Atomic %
Point 1	Zr	2.88
	Pt	97.12
Point 2	Zr	21.57
	Pt	78.43
Point 3	Zr	25.68
	Pt	74.32

based on AAO substrates considering the uniform and conformal nature of PEALD films even on porous substrates.

## Acknowledgments

This work was supported by the Global Frontier R&D Program on Center for Multiscale Energy System funded by the National Research Foundation under the Ministry of Science, ICT & Future Planning, Korea (2015M3A6A7065442). The IAMD at Seoul National University and BK21 plus is also acknowledged for their partial support.

## Appendix A. Supplementary data

Supplementary data related to this article can be found at <http://dx.doi.org/10.1016/j.ijhydene.2016.04.092>.

## REFERENCES

- [1] Steele BCH. Fuel-cell technology: running on natural gas. *Nature* 1999;400:619–21. <http://dx.doi.org/10.1038/23144>.
- [2] Service RF. Bringing fuel cells down to earth. *Science* 1999;285(80):682–5. <http://dx.doi.org/10.2307/2898473>.
- [3] Shim JH, Chao CC, Huango H, Prinz FB. Atomic layer deposition of yttria-stabilized zirconia for solid oxide fuel cells. *Chem Mater* 2007;19:3850–4. <http://dx.doi.org/10.1021/cm070913t>.
- [4] Duan C, Tong J, Shang M, Sanders M, Ricote S, Hayre RO. Readily processed protonic ceramic fuel cells with high performance at low temperatures. *Science* 2015;80:1–11. <http://dx.doi.org/10.1126/science.aab3987>.
- [5] Huang H, Nakamura M, Su P, Fasching R, Saito Y, Prinz FB. High-performance ultrathin solid oxide fuel cells for low-temperature operation. *J Electrochem Soc* 2007;154:B20. <http://dx.doi.org/10.1149/1.2372592>.
- [6] Su PC, Chao CC, Shim JH, Fasching R, Prinz FB. Solid oxide fuel cell with corrugated thin film electrolyte. *Nano Lett* 2008;8:2289–92. <http://dx.doi.org/10.1021/nl800977z>.
- [7] An J, Kim Y-B, Park J, Gür TM, Prinz FB. Three-dimensional nanostructured bilayer solid oxide fuel cell with 1.3 W/cm<sup>2</sup> at 450 °C. *Nano Lett* 2013;13:4551–5. <http://dx.doi.org/10.1021/nl402661p>.
- [8] Kerman K, Lai BK, Ramanathan S. Pt/Y<sub>0.16</sub>Zr<sub>0.84</sub>O<sub>1.92</sub>/Pt thin film solid oxide fuel cells: electrode microstructure and stability considerations. *J Power Sources* 2011;196:2608–14. <http://dx.doi.org/10.1016/j.jpowsour.2010.10.068>.
- [9] Shim JH, Kang S, Cha SW, Lee W, Kim YB, Park JS, et al. Atomic layer deposition of thin-film ceramic electrolytes for high-performance fuel cells. *J Mater Chem A* 2013;1:12695–705. <http://dx.doi.org/10.1039/c3ta11399j>.
- [10] Kang S, Heo P, Lee YH, Ha J, Chang I, Cha S-W. Low intermediate temperature ceramic fuel cell with Y-doped BaZrO<sub>3</sub> electrolyte and thin film Pd anode on porous substrate. *Electrochem Commun* 2011;13:374–7. <http://dx.doi.org/10.1016/j.elecom.2011.01.029>.
- [11] Ha S, Su P-C, Cha S-W. Combinatorial deposition of a dense nano-thin film YSZ electrolyte for low temperature solid oxide fuel cells. *J Mater Chem A* 2013;1:9645. <http://dx.doi.org/10.1039/c3ta11758h>.
- [12] Park J, Lee Y, Chang I, Lee W, Cha SW. Engineering of the electrode structure of thin film solid oxide fuel cells. *Thin Solid Films* 2015;584:125–9. <http://dx.doi.org/10.1016/j.tsf.2014.11.018>.
- [13] Chang I, Ji S, Park J, Lee MH, Cha SW. Ultrathin YSZ coating on Pt cathode for high thermal stability and enhanced oxygen reduction reaction activity. *Adv Energy Mater* 2015;5. <http://dx.doi.org/10.1002/aenm.201402251>. n/a – n/a.
- [14] Ji S, Cho GY, Yu W, Su PC, Lee MH, Cha SW. Plasma-enhanced atomic layer deposition of nanoscale yttria-stabilized zirconia electrolyte for solid oxide fuel cells with porous substrate. *ACS Appl Mater Interfaces* 2015;7:2998–3002. <http://dx.doi.org/10.1021/am508710s>.
- [15] Park J, Chang I, Paek JY, Ji S, Lee W, Cha SW, et al. Fabrication of the large area thin-film solid oxide fuel cells. *CIRP Ann – Manuf Technol* 2014;63:513–6. <http://dx.doi.org/10.1016/j.cirp.2014.03.065>.
- [16] Ji S, Chang I, Cho GY, Lee YH, Shim JH, Cha SW. Application of dense nano-thin platinum films for low-temperature solid oxide fuel cells by atomic layer deposition. *Int J Hydrogen Energy* 2014;39:12402–8. <http://dx.doi.org/10.1016/j.ijhydene.2014.02.081>.
- [17] Park T, Chang I, Cha SW. Augmentation method of triple phase boundary in thin film solid oxide fuel cell via physical vapor deposition. *J Nanosci Nanotechnol* 2013;13:7834–8. <http://dx.doi.org/10.1166/jnn.2013.8102>.
- [18] Hong S, Bae J, Koo B, Kim Y-B. High-performance ultra-thin film solid oxide fuel cell using anodized-aluminum-oxide supporting structure. *Electrochem Commun* 2014;47:1–4. <http://dx.doi.org/10.1016/j.elecom.2014.07.008>.
- [19] Chang I, Woo S, Lee MH, Shim JH, Piao Y, Cha SW. Characterization of porous Pt films deposited via sputtering. *Appl Surf Sci* 2013;282:463–6. <http://dx.doi.org/10.1016/j.apsusc.2013.05.153>.
- [20] O'Hayre R, Cha S-W, Colella W, Prinz FB. *Fuel cell fundamentals*. 2nd ed. New York: John Wiley & Sons; 2009.
- [21] Profijt HB, Potts SE, van de Sanden MCM, Kessels WMM. Plasma-assisted atomic layer deposition: basics, opportunities, and challenges. *J Vac Sci Technol A Vac Surfaces Film* 2011;29. <http://dx.doi.org/10.1116/1.3609974>. 050801.